

**Elucidating dissociation activation energies in
host-guest assemblies featuring fast exchange dynamics**

Ronit Shusterman-Krush,^a Laura Grimm,^b Liat Avram,^c

Frank Biedermann,^b and Amnon Bar-Shir^{*a}

^aDepartment of Organic Chemistry, Weizmann Institute of Science, Rehovot, 7610001,
Israel

^bInstitute of Nanotechnology (INT), Karlsruhe Institute of Technology (KIT), Hermann-
von-Helmholtz Platz 1, 76344 Eggenstein-Leopoldshafen, Germany

^cDepartment of Chemical Research Support, Weizmann Institute of Science, Rehovot,
7610001, Israel

*Corresponding Author: amnon.barshir@weizmann.ac.il

A. Materials

Chemicals

Cucurbit[7]uril was purchased from Strem chemicals; 2-bromo-2-chloro-1,1,1-trifluoroethane (halothane; G1) from Sigma Aldrich; 2-amino-3-(5-fluoro-1H-indol-3-yl) propanoic acid (5-fluorotryptophan; G2) from CHEM IMPEX INT'L INC; and 2-ethenoxy-1,1,1-trifluoroethane (fluroxene; G3) and berberine chloride (BC) from Alfa Aesar. All commercial chemicals were used without further purification.

2,7-Dimethyl-diazapyrenium diiodide (MDAP) was synthesized from 1,3,6,8-tetrahydro-2,7-dimethyl-2,7-diazapyrene, following the reported Se-oxidation procedure.¹⁻³

Phosphate buffer solutions

Sodium dihydrogen phosphate monohydrate was purchased from Merck; lithium chloride from Alfa Aesar; sodium chloride from bio-lab; potassium chloride from Merck; rubidium chloride from Chem-Impex; cesium chloride from Fisher Scientific; and ammonium chloride from Macron.

B. Phosphate Buffer Preparation

To a volumetric flask containing 150 mL D₂O was added 138 mg NaH₂PO₄·H₂O. Using a concentrated solution of NaOH, the buffer solution was titrated to pH=7.0-7.1. The volumetric flask was then filled to yield a 5 mM phosphate buffer of pH=7.0-7.1.

C. NMR Sample Preparation

CB7 was dissolved in either D₂O or phosphate buffer with an ion source (LiCl, NaCl, KCl, RbCl, CsCl, or NH₄Cl) to a final concentration of 140 mM for 1D-NMR and GEST experiments or of 4 mM for cation-NMR and cation-diffusion measurements. For each studied host:guest system, CB7 was diluted to a different concentration: 100 μM, 200 μM and 10 μM for CB7:G1, CB7:G2 and CB7:G3, respectively. To a 4 ml solution of CB7, 10 μl of G1, G2 or G3 were added, resulting in a final ratio of host:guest of 1:20, 1:25 and 1:500, respectively, for GEST experiments (~5 mM of guest), 1:10 for 1D NMR studies (0.5 mM CB7, ~5 mM of guest) and 1:2 for diffusion NMR studies (2 mM CB7, ~4 mM of the guest). The resulting host-guest solution (2.2 ml) was then transferred to a 5 mm NMR tube. The final concentration of the guest was determined by inserting a capillary containing a pre-calibrated sodium fluoride (NaF) solution in D₂O into the NMR tube. The

concentration of the guest, determined from the integration value of guest relative to the known integration value of the NaF-capillary, was found to be ~5 mM per sample.

D. NMR Setup

All NMR experiments were performed on a 9.4T AVANCEIII NMR spectrometer (Bruker, Germany), with the sample temperature stabilized at 298 K. Both the ^1H -NMR (400 MHz) and ^{19}F -NMR (376.7 MHz) spectra were acquired with 128 scans. T_1 and T_2 (^{19}F -NMR) of the various CB7:guest complexes in the different solutions were measured and then used in the Bloch simulations: The longitudinal (T_1) and transverse (T_2) relaxation times of a guest were calculated using inversion recovery (IR) and Car-Purcell-Meiboom-Gill (CPMG) experiments

E. Diffusion NMR setup

NMR diffusion measurements were performed using a gradient system capable of producing magnetic field pulse gradients in the z-direction of about 50 G cm^{-1} . ^1H -NMR (400 MHz) diffusion experiments were performed using the LED (longitudinal eddy current delay) diffusion sequence; the gradient duration (δ) was 4 ms and pulse gradient separation (Δ) was 40 ms. ^7Li -NMR (155.5 MHz) diffusion experiments were performed using the LED (longitudinal eddy current delay) diffusion sequence; the gradient duration (δ) was 4 ms and pulse gradient separation (Δ) was 60 ms. ^{23}Na - and ^{133}Cs -NMR diffusion experiments were performed using the PGSE (pulsed gradient spin echo) diffusion sequence; the gradient duration (δ) was 10 ms and 8 ms, and the pulse gradient separation (Δ) was 12 ms and 60 ms for ^{23}Na and ^{133}Cs , respectively.

F. CEST experiments

^{19}F -GEST data were acquired according to the following steps. A pre-saturation pulse (t_{sat}) with a length of 3 sec was applied prior to the 90° RF pulse. The saturation pulse strength B_1 was set for each experiment as mentioned in the text or in the figure captions. The frequency of the pre-saturation pulse was swept from $\Delta\omega = +6.1$ ppm to $\Delta\omega = -6.1$ ppm in 100 Hz = 0.27 ppm steps relative to the resonance of the free guest (set to 0 ppm for convenience). In addition, a ^{19}F spectrum was acquired with the pre-saturation pulse applied at $\Delta\omega = +73.9$ ppm as a reference spectrum (S_0). For each frequency offset ($S_{\Delta\omega_i}$), the data were acquired with eight scans, using a repetition time of 15 sec, resulting in an

experimental time of ~2 min per ^{19}F spectrum and a total CEST experiment time of ~1 h 44 min.

G. CEST Simulations

For k_{out} estimations of each of the studied host-guest systems, the multipower z-spectra obtained from all the experiments was compared to an analytical solution of the Bloch-McConnell equation describing the expected z-spectrum. Saturation powers for all experiments were varied between 25 Hz and 200 Hz and are described in detail for each CEST experiment in the figures. The code for the simulations can be found at <http://www.cest-sources.org/doku.php?id=start>.

H. Bloch-McConnell data fitting

For k_{out} estimations of the studied host-guest systems in different solvents, the z-spectra of multi B_1 CEST experiments were fitted using the Bloch-McConnell equations, as recently described^{4, 5}. The saturation powers used for all experiment were (25, 50, 100, 150 and 200) Hz. Both numerical and analytical simulations (yielding similar k_{ex} values) were performed on the z-spectra using custom-written scripts in MATLAB version 8.2.0.701 (The MathWorks, Natick, MA). The code for data fitting can be found at <http://www.cest-sources.org/doku.php?id=start> and follows the publication by Zaiss and Bachert.^{6, 7}

I. ITC Sample Preparation

A stock solution of 1 mM CB7 was prepared in 5 mM phosphate buffer with an ion source (LiCl, NaCl, KCl, RbCl, or CsCl) to reach a final salt concentration of 140 mM (pH~7). A stock solution of G3 dissolved in the same solvent mixture was prepared according to the preparation scheme described in section B to predetermine the guest concentration using ^{19}F -NMR measurements.

J. ITC Setup

All ITC experiments were performed using a MicroCal PEAQ-ITC (Malvern Panalytical) at 298 K. CB7 was transferred to the sample cell (320 μl) and the ^{19}F -guest was transferred to the syringe (38 μl). The number of injections in each experiment was set to 26 injections with an injection volume of 1.5 μl per injection (the first injection was 0.4 μl). The CB7

concentration was set to 0.5 mM and the guest concentration was ~5 mM. For parameter determination the ITC data was analyzed by the Malvern instrument software with the one-set-of-sites model and the first data point was always omitted. The data was baseline corrected by the average heat value obtained by the titration of guest into water.

K. Activation Energy Calculation

Four subsequent ^{19}F -CEST measurements were acquired at four different temperatures. Each data set was analyzed according to section G to extract the corresponding k_{out} value for each temperature. For each sample, the natural logarithm of the k_{out} value was plotted as a function of the inverse temperature according to the Arrhenius equation (eq. 1) and the dissociation activation energy value ($E_{\text{a,out}}$) was extracted from the slope. The reported errors for the calculated $E_{\text{a,out}}$ (Table 1) values were evaluated based on the error obtained for the $k_{\text{ex,out}}$ values at each experimental temperature. To this end, $E_{\text{a,out}}$ values were evaluated by plotting a series of $\text{mean}(k_{\text{ex,out}})$ values, a series of $\text{mean}(k_{\text{ex,out}}) + \text{error}(k_{\text{ex,out}})$ and a series of $\text{mean}(k_{\text{ex,out}}) - \text{error}(k_{\text{ex,out}})$. The three values were averaged to denote $\text{mean } E_{\text{a,out}} \pm \text{error}$. (For the samples of CB7:G3 with either Li^+ or Rb^+ four $k_{\text{ex,out}}$ values obtained from experiments performed at four different temperatures were used for the error evaluation. For the samples of CB7:G3 with Na^+ three $k_{\text{ex,out}}$ values obtained from experiments performed at three different temperatures were used for the error evaluation).

The energy ($E_{\text{a,in}}$) was evaluated from the following equation:

$$\Delta H = E_{\text{a,in}} - E_{\text{a,out}} \quad (\text{Equation S1})$$

ΔH – Reaction enthalpy extracted from ITC measurement.

L. Dissociation free energy calculation

In the Eyring equation, the Gibbs free energy (ΔG) describes the free energy of a transition state (ΔG^\ddagger). This free energy is dependent on the enthalpy (ΔH^\ddagger) and entropy (ΔS^\ddagger):

$$\Delta G^\ddagger = \Delta H^\ddagger - T \Delta S^\ddagger \quad (\text{Equation S2})$$

Assuming a unimolecular, one-step reaction, the Arrhenius parameters (E_a and A) from section K can be correlated to the enthalpy and entropy of the transition state according to the following equations (with the errors evaluated based on the errors obtained for $E_{a,out}$):

$$E_a = \Delta H^\ddagger + RT \quad (\text{Equation S3})$$

$$A = (k_B T/h) \cdot \exp(1 + \Delta S^\ddagger/R) \quad (\text{Equation S4})$$

ΔH^\ddagger - Enthalpy of transition state [kJ/mol]

ΔS^\ddagger - Entropy of transition state [kJ/mol]

T – Temperature in Kelvin [K]

R - Universal gas constant (8.3145 JK⁻¹mol⁻¹)

k_B - Boltzmann constant (1.381x10⁻²³ JK⁻¹)

h - Planck constant (6.63x10⁻³⁴ Js)

M. Steady-State Fluorescence and Stopped-Flow Experiments

The concentration of CB7 was determined by titration with MDAP. For berberine, MDAP and F-tryptophan the concentrations were determined by using their molar extinction coefficient (berberine: 22500 M⁻¹ cm⁻¹ at 344 nm, MDAP: 7800 M⁻¹ cm⁻¹ at 393 nm and F-tryptophan: 5600 M⁻¹ cm⁻¹ at 280 nm) on a Jasco V-730 UV-Vis/NIR spectrophotometer. Fluorescence measurements were performed on a Jasco FP-8300 fluorescence spectrometer equipped with a 450 W xenon arc lamp, double-grating excitation and emission monochromators. In the course of the optical titrations, all concentrations were kept constant except for that of the titrant. Binding constants were determined by using a 1:1 complexation model.

Stopped-flow measurements were conducted with a SFA-20 rapid kinetic accessory with a pneumatic drive unit from HI-TECH Scientific connected to a Jasco FP-8300 fluorescence spectrometer equipped with a 450 W xenon arc lamp, double-grating excitation and emission monochromators. The reactants were mixed in 1:1 volume ratio at 298 K. The temperature was controlled with a Julabo F25-ED thermostat. All spectral experiments were conducted under air at ambient temperature in Millipore-grade H₂O. Stopped flow traces were fitted to the numerical solution of differential equation describing the time dependence of the fluorescence intensity to calculate the rate constant of inclusion (k_{in}).

N. SI Figures

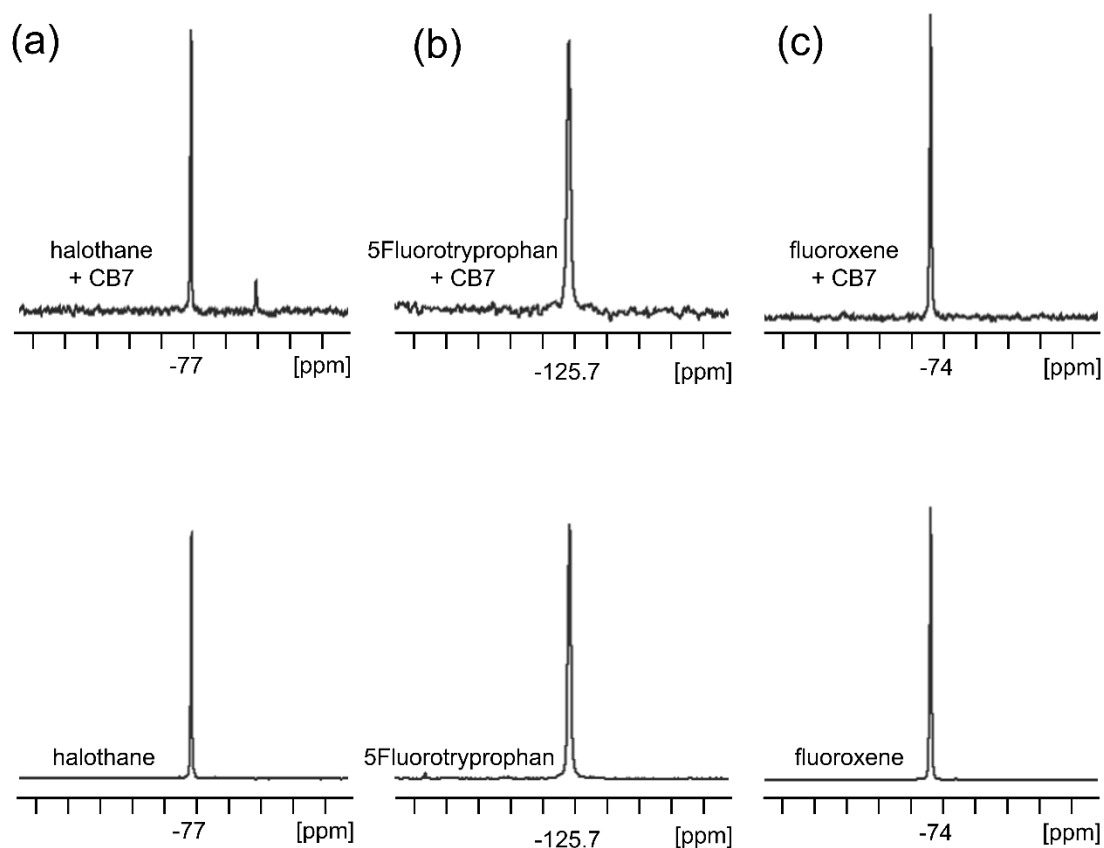


Figure S1. ^{19}F -NMR spectra of the supramolecular complexes of CB7 and (a) halothane (G1), (b) 5-fluorotryptophan (G2), and (c) fluoroxene (G3) at a molar ratio of 1:10 in 5 mM phosphate buffer (pH=7).

phosphate buffer

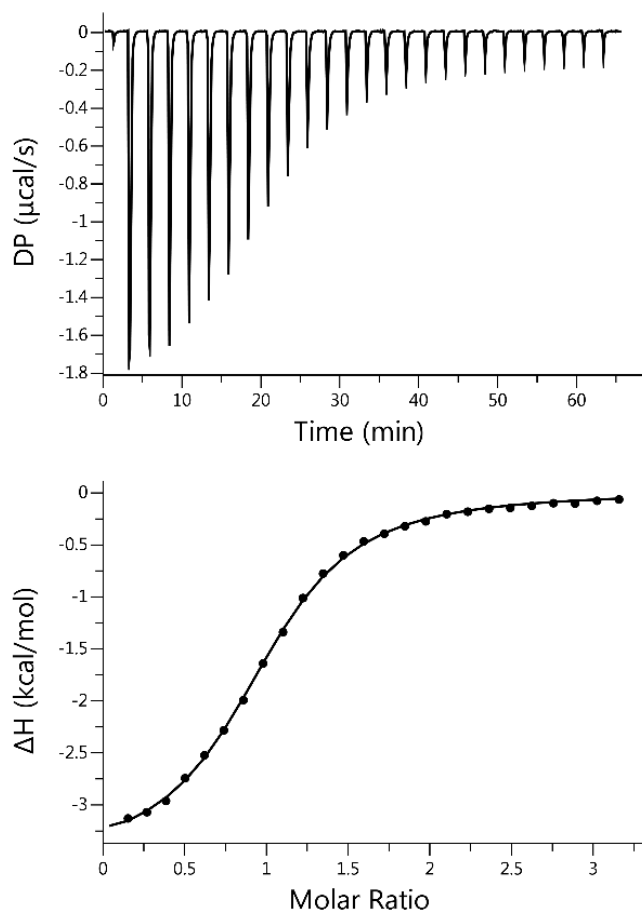


Figure S2. Isothermal titration calorimetry data for the CB[7]:G3 complex in 5 mM phosphate buffer without the addition of further salts.

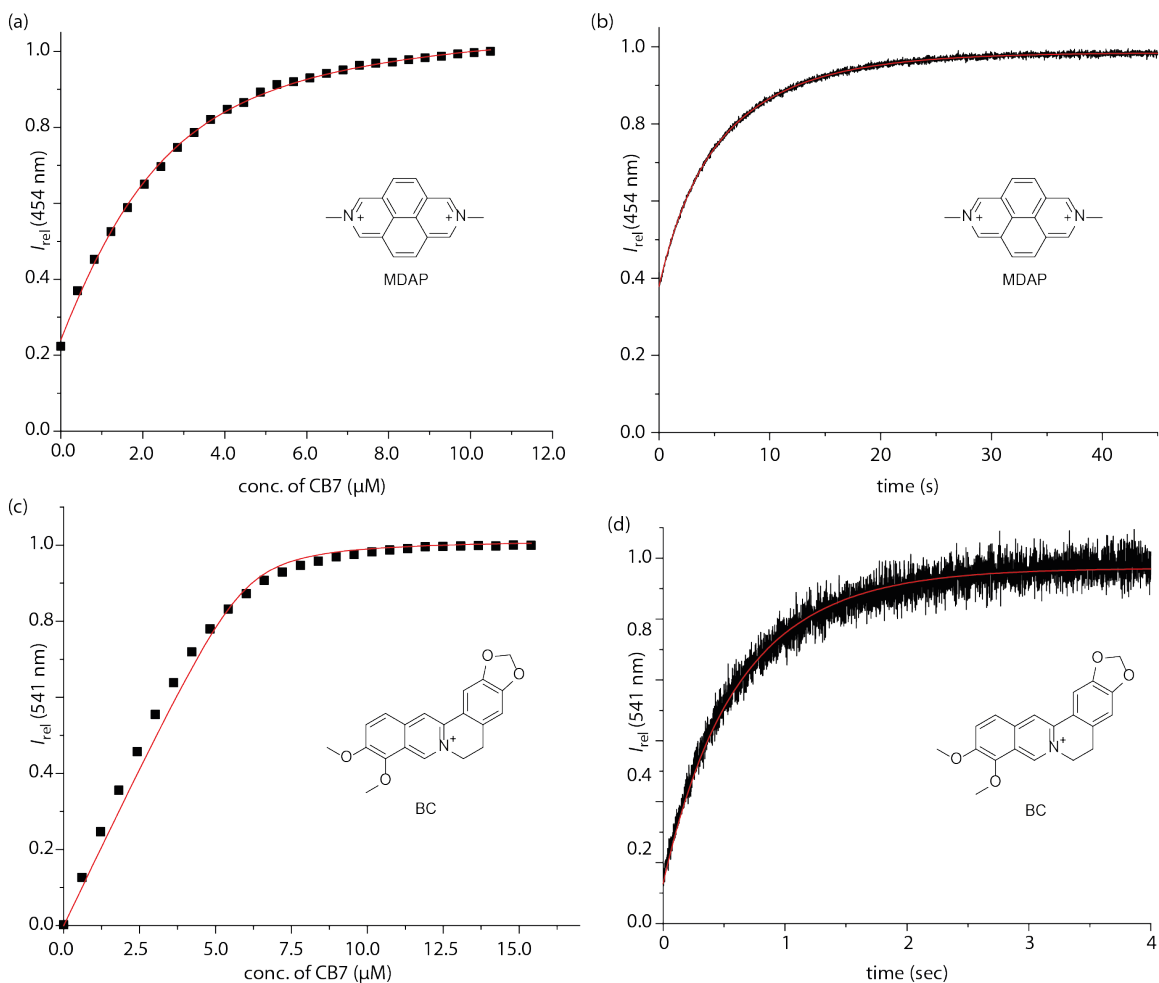


Figure S3. (a) Normalized binding curve for MDAP (2 μM) with CB7 (0-12 μM) in 140 mM NaCl and 5 mM phosphate buffer ($\lambda_{\text{ex}} = 338$ nm). (b) Normalized stopped-flow signal at 454 nm for the mixing of a 10 μM MDAP solution and a 10 μM CB7 solution in 140 mM NaCl and 5 mM phosphate buffer ($\lambda_{\text{ex}} = 357$ nm). Initial concentrations at $t = 0$ sec were 5 μM . The red lines represent the result of the nonlinear least-square analysis. (c) Normalized binding curve for BC (6 μM) with CB7 (0-15.5 μM) in 0.001 M HCl (pH 3; $\lambda_{\text{ex}} = 421$ nm). (b) Normalized stopped flow signal at 541 nm for the mixing of a 0.4 μM BC solution and a 0.2 μM CB7 solution in 0.001 M HCl ($\lambda_{\text{ex}} = 421$ nm). Initial concentrations at $t = 0$ sec were 0.1 μM CB7 and 0.2 μM BC. The red lines represent the result of the nonlinear least-square analysis.

Table S1. Binding constants (K_A) and rate constants (k_{in}) for the inclusion of the here used dyes into CB7. Estimated errors are 20% in K_A , k_{in} and k_{out} .

Buffer System	dye	$K_A / \cdot 10^6 \text{ M}^{-1}$	$k_{\text{in}} / \cdot 10^3 \text{ M}^{-1} \text{ s}^{-1}$	$k_{\text{out}} / \text{s}^{-1}$
5 mM phosphate buffer, 140 mM LiCl	MDAP	12	281	0.023
5 mM phosphate buffer, 140 mM NaCl	MDAP	1.0	30	0.03
Millipore-grade H₂O⁸	BC	18	19100	0.81
0.001 M HCl	BC	9.0	4960	0.53

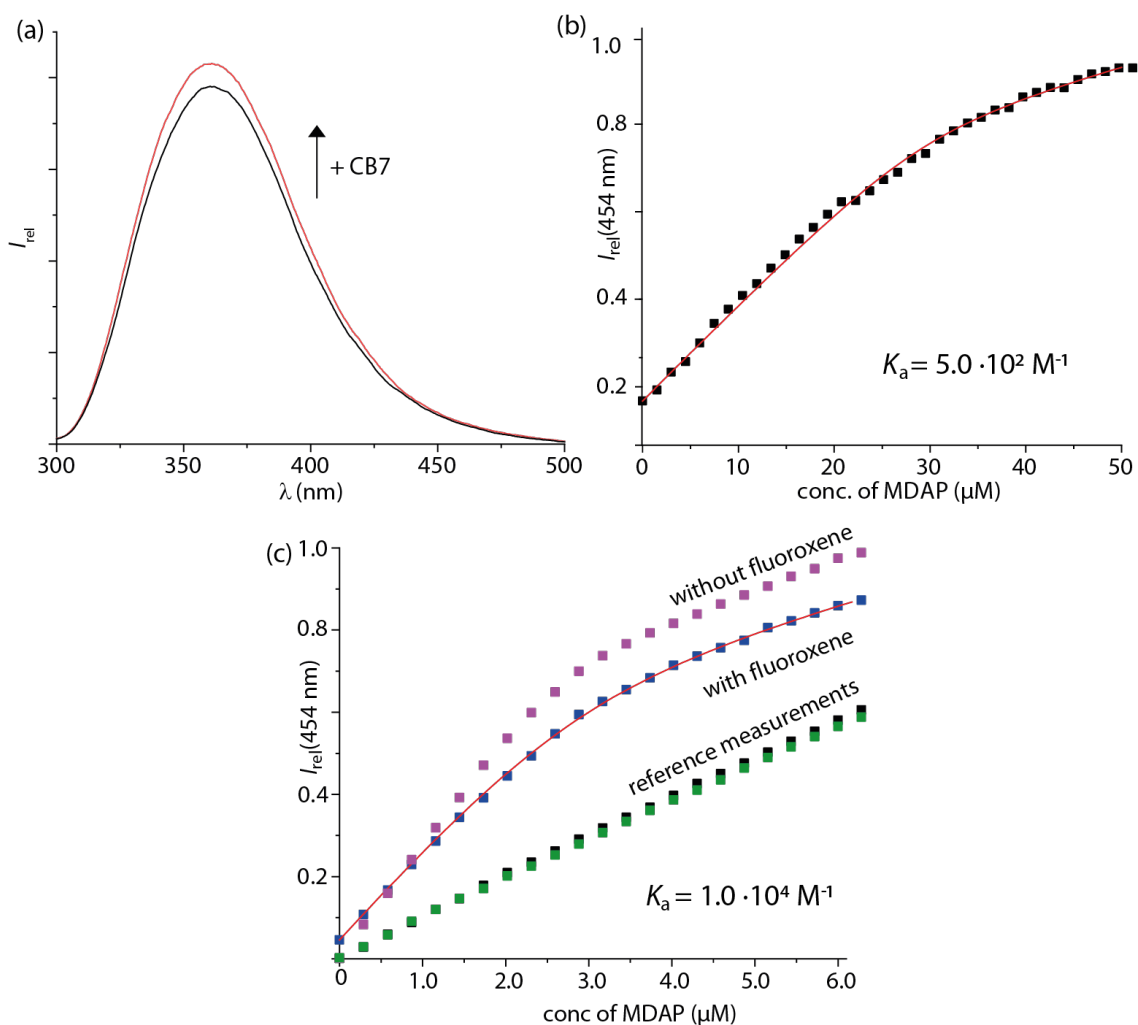


Figure S4. (a) Steady-state spectra of F-tryptophan ($30 \mu\text{M}$) in 5 mM sodium phosphate buffer with 140 mM NaCl with (red) and without (black) CB[7] ($30 \mu\text{M}$). (b) Determination of the binding constant of F-tryptophan to CB7 by guest displacement assay (GDA) in 5 mM sodium phosphate buffer with 140 mM NaCl. Due to the small intensity change upon the binding of 5-fluorotryptophan to CB7 a direct binding assay was not suitable for the determination of the binding constant. (c) Determination of the binding constant of fluoroxene to CB7 by guest displacement assay (GDA) in 5 mM sodium phosphate buffer with 140 mM NaCl (blue). As references the titration of MDAP into a solution of CB7 in the buffer mixture (pink), into the buffer mixture alone (black) and into the buffer mixture with additional fluoroxene (green) are shown. As excitation wavelength $\lambda_{ex} = 357 \text{ nm}$ was used. Corresponding dye values can be found in Figure S3.

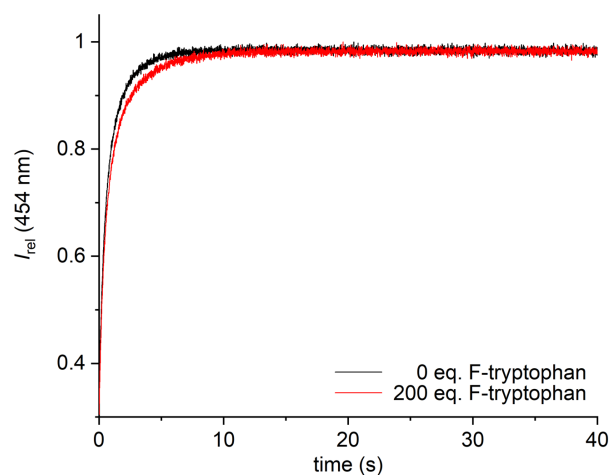


Figure S5. Representative GDA kinetic binding curve determined by fluorescence intensity variations for the mixing of 10 μM MDAP solution and 10 μM CB7 with (black) and without (red) the addition of 200 eq. F-tryptophan (10 mM) in 5 mM phosphate buffer and 140 mM NaCl. The kinetics cannot be fitted reliably due to the fast kinetics of F-tryptophan binding to CB7 and therefore stopped-flow is not a good method for the kinetics determination for this host-guest system ($\lambda_{\text{ex}} = 421 \text{ nm}$). Similar results were found upon the addition of 140 mM LiCl to the buffer solution.

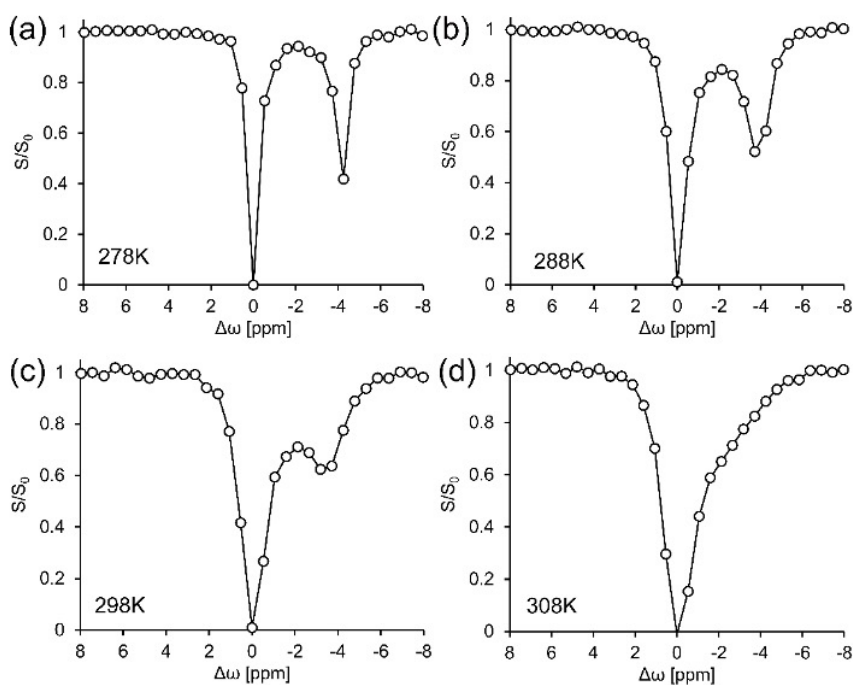


Figure S6. Experimental z-spectra of CB7:G2 (1:50 ratio) in 5 mM phosphate buffer solution at different temperatures: (a) 278K, (b) 288K, (c) 298K and (d) 308K.

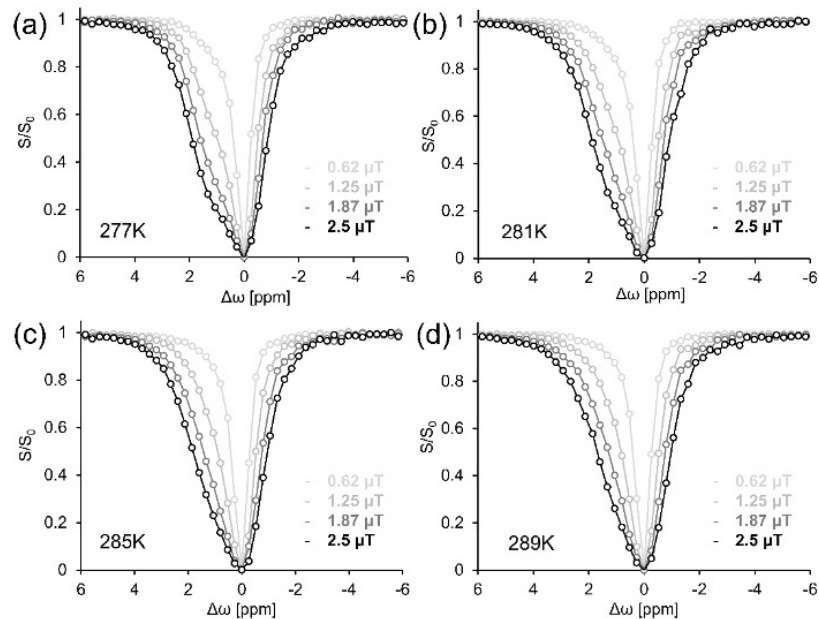


Figure S7. Experimental z-spectra of multi-power GEST experiments performed on CB7:G3 (1:100 ratio) complex in 5 mM phosphate buffer solution at different temperatures: (a) 277K, (b) 281K, (c) 285K and (d) 289K.

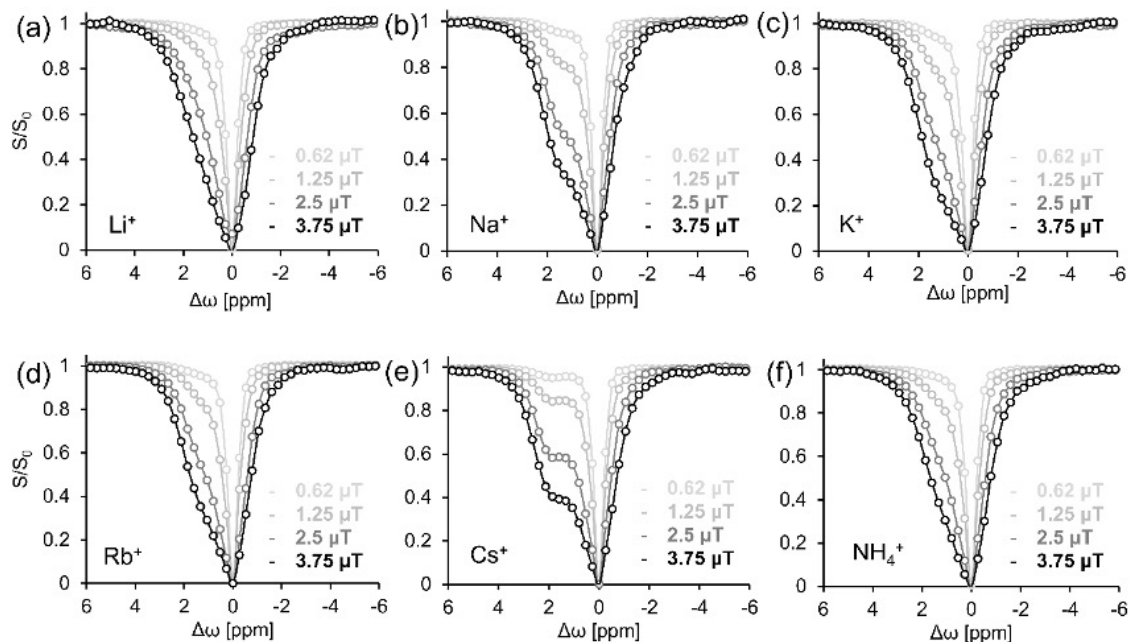


Figure S8. The effect of monovalent cations on guest dissociation exchange rates. Experimental z-spectra of multi-power GEST experiments performed on the CB7:G3 complex at a molar ratio of 1:500 in 5 mM phosphate buffer solution with the addition of 140 mM (a) LiCl, (b) NaCl, (c) KCl, (d) RbCl, (e) CsCl and (f) NH₄Cl.

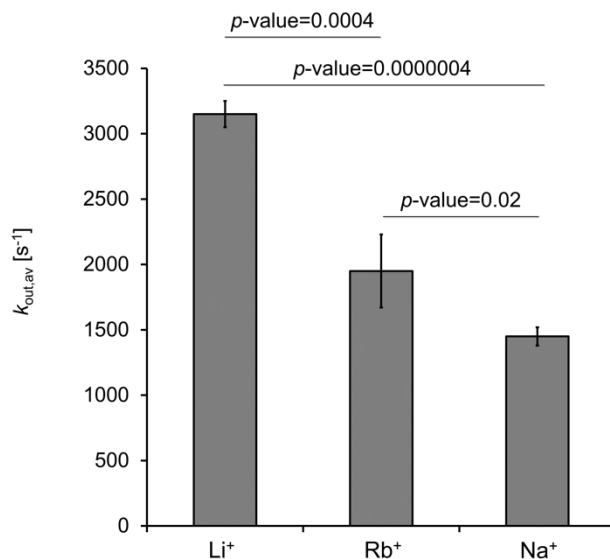


Figure S9. Dissociation exchange rates (k_{out} , s^{-1}) of CB7:G3 solution in the presence of monovalent cations. Averaged dissociation exchange rates (k_{out} , s^{-1}), of phosphate buffer solution of CB7:G3 (1:100 ratio) in the presence of various monovalent cations (Li^+ , Rb^+ and Na^+) added as 140 mM of LiCl, RbCl and NaCl to the 5 mM phosphate buffer solution. The averaged $k_{out,av}$ values were calculated from four independent experiments (N=4, different samples, independently prepared prior each experiment) performed for each solution. Dissociation exchange rates were evaluated from a single B_1 GEST experiment (100 Hz) by using the Bloch–McConnell simulations with a two-pool model. Error bars represent standard deviations (N=4). Statistics: paired two-tailed Student’s t-test with obtained p-values denoted in the figure.

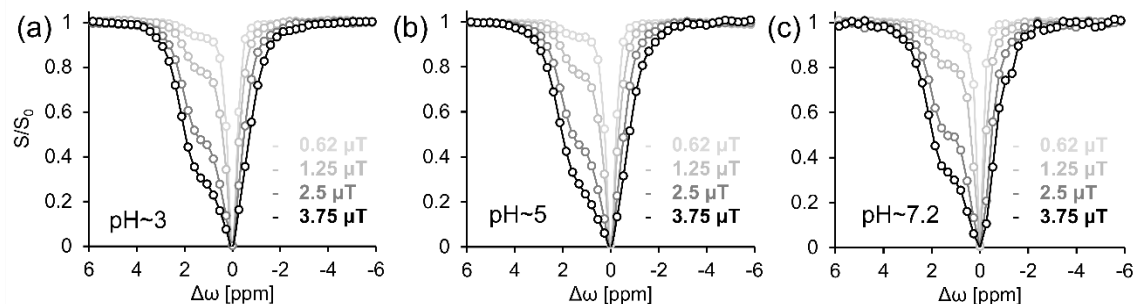


Figure S10. The Na^+ effect on the guest dissociation rates at different pH values. Experimental z-spectra of multi-power GEST experiments performed on the CB7:G3 complex at a molar ratio of 1:500 in 5 mM phosphate buffer solution with 140 mM NaCl at (a) pH~3, (b) pH~5 and (c) pH~7.2.

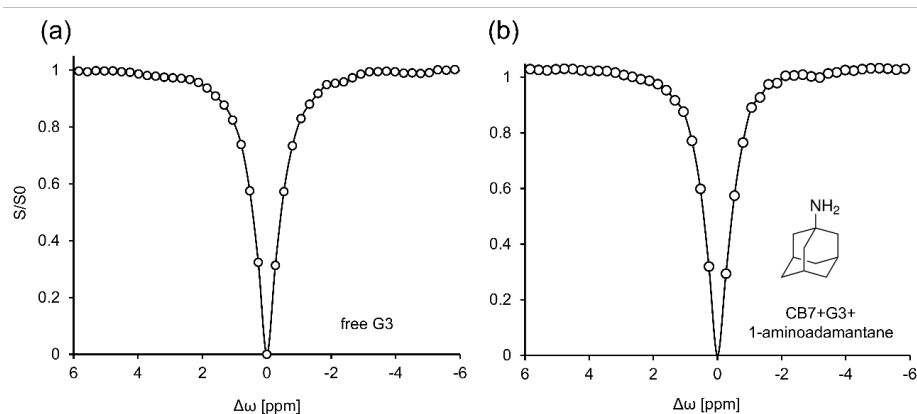


Figure S11. Experimental z-spectra of CB7:G3 complex in 5 mM phosphate buffer (a) with and (b) without the addition of 1-aminoadamantane at a molar ratio of 1:1:100 (CB7:1-aminoadamantane:G3).

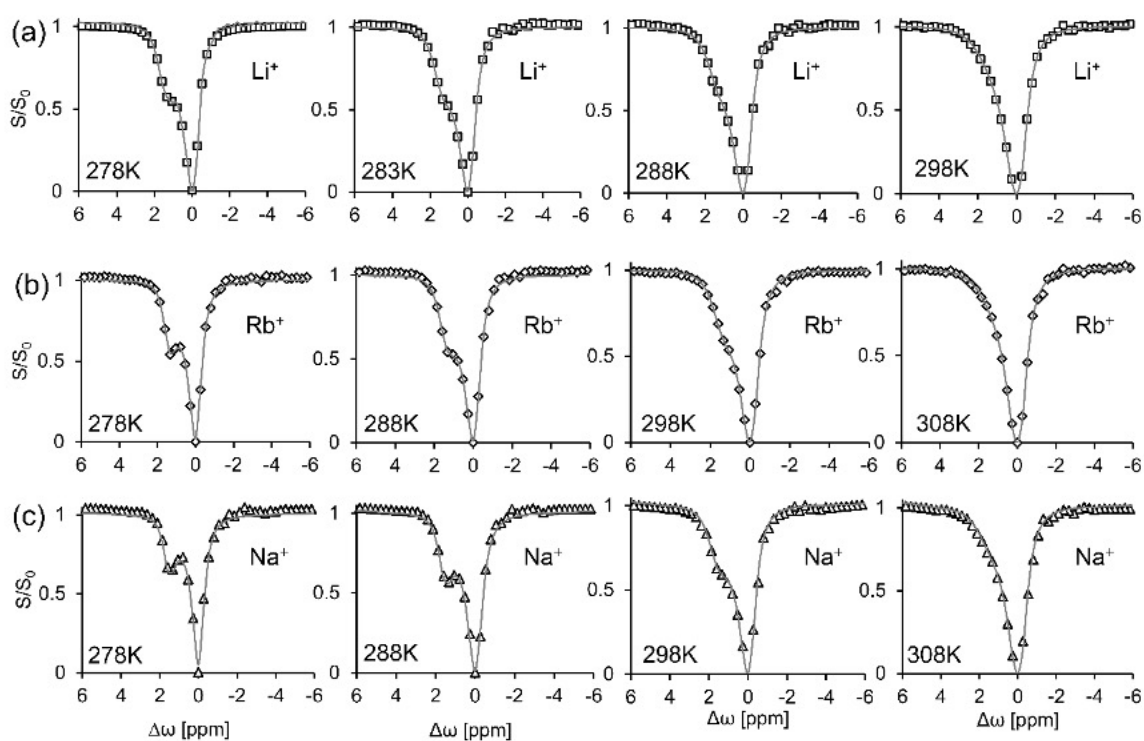


Figure S12. Experimental z-spectra of the CB7:G3 complex at a molar ratio of 1:500 in 5 mM phosphate buffer with 140 mM (a) LiCl, (b) RbCl and (c) NaCl at different temperatures: 278K, 283K, 288K, 298K and 308K.

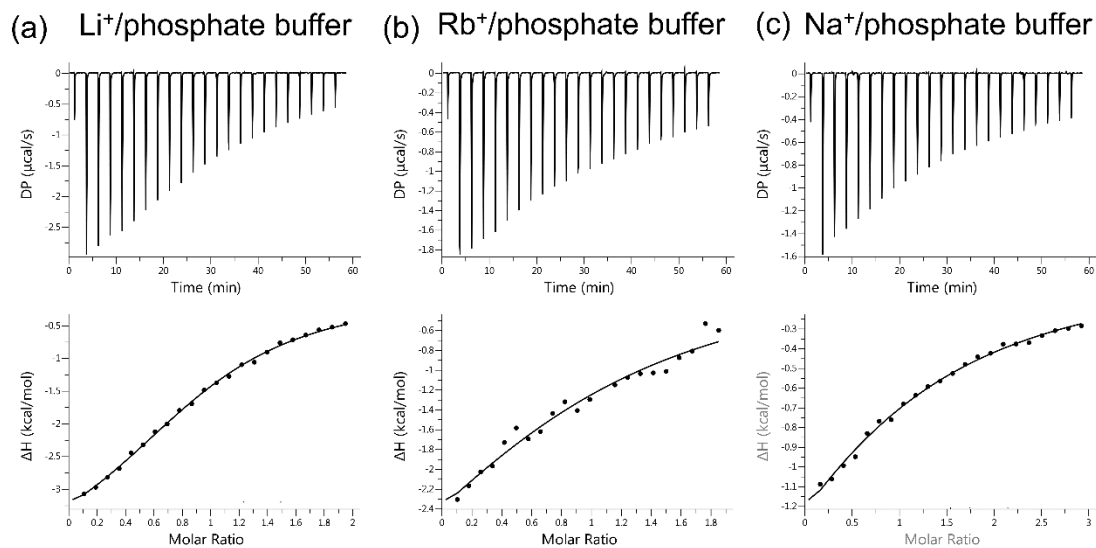


Figure S13. Isothermal titration calorimetry data for the CB7:G3 complex dissolved in 5 mM phosphate buffer with the addition of 140mM (a) LiCl (b) RbCl, and (c) NaCl.

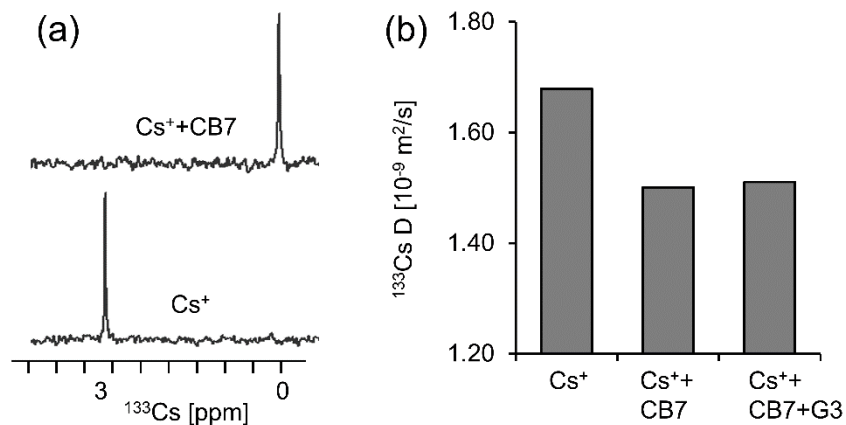


Figure S14. (a) ¹³³Cs-NMR with (upper panel) and without (lower panel) 2mM CB7. (b) ¹³³Cs-diffusion coefficients in 5 mM phosphate buffer containing free M⁺, M⁺•CB7 at a molar ratio of (2:1), and M⁺•CB7•G3 at a molar ratio of (2:1:2) (total M⁺ concentration equals 4 mM).

O. References

1. A. N. Basuray, H.-P. Jacquot de Rouville, K. J. Hartlieb, T. Kikuchi, N. L. Strutt, C. J. Bruns, M. W. Ambrogio, A.-J. Avestro, S. T. Schneebei, A. C. Fahrenbach and J. F. Stoddart, *Angew. Chem. Int. Ed.*, 2012, **51**, 11872-11877.
2. A. J. Blacker, J. Jazwinski and J.-M. Lehn, *Helv. Chim. Acta*, 1987, **70**, 1-12.
3. K. J. Hartlieb, L. S. Witus, D. P. Ferris, A. N. Basuray, M. M. Algaradah, A. A. Sarjeant, C. L. Stern, M. S. Nassar, Y. Y. Botros and J. F. Stoddart, *ACS Nano*, 2015, **9**, 1461-1470.
4. L. Avram, V. Havel, R. Shusterman-Krush, M. A. Iron, M. Zaiss, V. Sindelar and A. Bar-Shir, *Chem. Eur. J*, 2019, **25**, 1687-1690.
5. M. Zaiss, G. Angelovski, E. Demetriou, M. T. McMahon, X. Golay and K. Scheffler, *Magn. Reson. Med.*, 2018, **79**, 1708-1721.
6. M. Zaiss and P. Bachert, *NMR Biomed*, 2013, **26**, 507-518.
7. M. Zaiss, Z. Zu, J. Xu, P. Schuenke, D. F. Gochberg, J. C. Gore, M. E. Ladd and P. Bachert, *NMR Biomed.*, 2015, **28**, 217-230.
8. S. Sinn, A. Prabodh, L. Grimm, Z. Miskolczy, M. Megyesi, L. Biczok, S. Bräse and F. Biedermann, *Chem. Commun.*, 2020, **56**, 12327-12330.